RSC Advances

ROYAL SOCIETY OF CHEMISTRY

www.rsc.org/advances

Synthesis of 3-Dimensional porous graphene nanosheets using electron cyclotron resonance plasma enhanced chemical vapour deposition

Rajesh Thomas, G Mohan Rao
Dept. Of Instrumentation and Applied Physics
Indian Institute of Science, Bangalore, India
thomasphy@gmail.com

Abstract

Microwave plasma driven chemical vapour deposition were used to synthesize graphene nano sheets from the mixture of Acetylene and Hydrogen gas molecules. In this plasma, Acetylene decomposes to carbon atoms that form nanostructures in the outlet plasma stream and gets deposited on the substrate. The GNS consists of few layers of graphene that aligned vertical to the substrate. The graphene layers has been confirmed by high-resolution transmission electron microscopy and Raman spectral studies were conducted to shows the defective nature of the sample. The growth of nano sheets in vertical direction is assumed due to the effect of electric field and from the difference in deposition rate of axial and parallel direction. These vertical graphene sheets attracted for various applications in energy storage and sensors.

1. Introduction

Carbon materials are getting much attention in the recent years due to their unique properties, in various forms such as diamond, graphite, graphene, amorphous carbon, fullerenes and nanotubes. These structures have shown remarkable differences in properties and hence in potential applications such as photovoltaic [1-4], field emition [5], energy storage [6], transisters [7], biology [8], hydrogen storage [9] etc. due to their peculiar properties of chemical, electrical, optical and mechanical properties [10].

There are several methods for synthesizing graphene, which can be broadly classified as top down and bottom up approaches. In bottom up technique, graphene is synthesized from atomic or molecular species, whose precursor particles were allowed to gradually grow in size. In top down synthesis, graphite, carbon fibers and carbon nanotubes are the starting materials and individual graphene layers are extracted or peeled off either by physical, electrochemical or chemical methods [11-14]. The road block in making graphene devises is the absence of a viable method for mass production. Chemical vapour deposition (CVD) [15], mechanical exfoliation [16], chemical exfoliation [17], liquid phase exfoliation [18] and epitaxial growth [19] generally produce single, bi-layer or tri-layer graphene sheets, but have low yield and hence unsuitable for mass production. Recently, graphene has been synthesized from chemical routes [20] in which, graphite oxide readily exfoliates in water and this suspension can be chemically reduced to yield graphene. This highly reproducible chemical route is among the first techniques to promise mass production of graphene. But the synthesis of graphene through chemical rout, which includes many toxic chemicals, is not compatible with the present microelectronic device technology.

Vertically oriented graphene (VG) nanosheet is a special kind of two dimensional nanostructure oriented vertically on a substrate. Theses VG nanosheets are highly porous and consists of few leyer graphene with a layer number of 1-15 and the porous diameter is in the range of 50 to 200nm. These carbon nanostructures have unique features such as sharp edges, vertical morphology, high surfacr to volume ratio etc. and can be found in great applications in energy storage (Li Ion batteries [21, 22] and super capacitor), gas sensor, field emiters, bio sensors and fuel cell. [1-10]

Microwave plasma enhanced chemical vapour deposition (MW-PECVD) is established as a key method to produce graphene nanosheet. PECVD technique has many advantages over thermal CVD includes low substrate temperature, higher growth selectivity, better control in nano structure ordering [23], low operating pressure (10^{-3}- 10^{-4} mbar) leading to high purity films, high ionization coefficient enabling higher growth rate [24-27].

1.2 Experimental

Graphene nanosheet was synthesized in a home-made ECR-PECVD set-up (Fig. 1). The ECR system consisted of a plasma source chamber mounted on to a stainless steel chamber. The beam diameter at the exit of the source is about 100 mm. A flexible substrate holder allows free positioning of substrate along the axis of the source chamber. The substrate was kept at 10 cm away from the exit of plasma source and the ion density at the surface of substrate was measured approximately 9.5x 10^{10} cm^{-3}. The details of the experimental system and working principle have been described in our group's previous paper [28].

Copper (Cu) foil of 0.25 mm thick (Alfa Aesar), annealed, poly crystalline and area of $1cm^2$ has been used as the substrate. The substrate was cleaned with dilute nitric acid and rinsed with de-ionized (DI) water. Prior to the deposition, substrate was heated at 500^0C for 30 minute. After that the substrate was treated in H_2 plasma for 10 min at 500^0C. The carbon deposition was carried out at 700^0C for 30 minute. A mixture of Hydrogen (H_2) and Acetylene (C_2H_2) was used at a ratio of 2:1. The plasma power was set to 500 W and the working pressure was at 7x10^{-4} mbar. Further, GNS was deposited over different substrates such as Platinum or Nickel coated copper, SiC, SiO_2 and Quartz.

1.3 Results and discussion

1.3.1 Growth of Graphene nanosheet

Several reports have been published for the synthesis of graphene nanosheet. Wu [25] and Zheng et al [23] described the synthesis of graphitic carbon nanostructure composed of a few layers of graphene vertically standing on a substrate via microwave plasma enhanced chemical vapor deposition (MW-PECVD). J Chen et al. reported the GNS synthesis using direct current (dc) PECVD at atmospheric pressure on various substrates [29-31]. The exact mechanism in the GNS growth is not known completely.

The verticality of GNS may be due to the differenc of growth in horizontal to vertical diretions. The excat mechanism of GNS growth is not well understood, and it has assumed that electric field plays an important role [32, 33]. There are reported, electric field plays an important role in the alignment of CNTs in microwave plasmas [34, 35]. The electric field tend to align vertically to the plate, when metallic objects directly placed in the plasma field even without any biasing. In our experiment we placed the substrate over a metallic plate from where the electric field can influences the GNS growth. Not only the electric field that affecting the verticality, but also the H_2 dilution also contributing to shape the nano wall morphology by etching the loosely bonded carbon toms and amorphous carbon. And hence the graphitization of graphene nano wall can be enhanced.

From the SEM observations, it was found that, an amorphous carbon film was deposited on the Cu substrates from the acetylene plasma. At certain temperature, in the presence of plasma, the amorphous carbon film was bombarded to form the random small size nanoflakes. These nanoflakes act as the nucleation site. Subsequently, the GNS grew on the nucleation positions and aligned vertically on the substrate. The verticality of GNS is due the

difference in growth rates between directions of parallel and perpendicular to the graphene nanosheet [36]. The local electric field from the plasma also has the effect in vertical orientation of GNS. The electric-field dependent orientation has been observed for carbon nanotube and nanowall [37, 38]. Here we are studying the growth of GNS films by various growth parameters and look into how that influence the growth such as deposition time, flow rate of acetylene, temperature and microwave power. The hydrogen dilution with acetylene plasma also has influence in growth of GNS.

Various parameters influences the growth of graphene sheet for the plasma CVD deposition. The surface morphology of GNS over cu substrate at different deposition time is given in fig.2. All the depositions were carried out at 500 W microwave powers and at a substrate temperature of 700^0C. The flow rate of acetylene was set to 12.4 sccm and the ratio of C_2H_2:H_2 is 1:2. After one min of deposition, no GNS nucleation was observed (fig.2a). An amorphous kind of carbon was deposited after 3min of deposition (fig.2b). Then uniform nucleation of GNS was started after 5 min of deposition (fig.2c). From the SEM observations, it was found that the nucleation started after some time of deposition. The thickness of the GNS film was about 200 nm (fig 2d).

Fig.3 shows the SEM images of GNS grown by varying the flow rate of C_2H_2. All the depositions were carried out at 500 W microwave power, 700^0C of substrate temperature and 5 min of deposition time. At the flow rate of 5sccm of C_2H_2, an amorphous carbon deposited on the substrate and the GNS formation was not visible (fig 3a). When the flow rate was increased to 12 sccm, nucleation of GNS started (fig.3b) and at 25 sccm, there was good GNS formation on the substrate (fig. 3c) and the GNS was highly porous and uniformly distributed. The mixture of C_2H_2 and H_2 has been taken as 1:2. There should be a minimum concentration of C_2H_2 required to get uniform GNS over the entire substrate.

The SEM images (fig. 3d-f) shows the effect of microwave power on the growth of GNS. The microwave power varied from 100 W to 500 W. For the deposition of GNS, the flow rate of C_2H_2 was kept constant at 12 sccm. All the deposition was carried out at a substrate temperature of 700^0C and 5 minuts of deposition time. Further, at 100 W microwave power (fig.3d), the GNS film contains mainly amorphous carbon. When the microwave power increased to 300 W, nucleation of GNS started (fig. 3e) and at 500 W, well defined GNS growth were observed (fig. 3f). The growth of GNS at different temperature was studied at constant flow rate of C_2H_2 at12 sccm, microwave power of 500W and 5 minutes of deposition time. At room temperature deposition, the film contains irregular and amorphous carbon were shown in (fig. 3g). When the temperature increased to 400^0C and also at 700^0C, there was uniform distribution and nucleation of GNS started to observe (fig 3h and 3i).

Nonomura et al. studied the effect of H_2 dilution in GNS growth by hot wire CVD. It was found that, GNS growth varies with different hydrogen dilution with methane (CH_4). The surface morphology of GNS changes at different hydrogen concentration. One of the effects of H_2 dilution would be the etching activity of the hydrogen radical. The hydrogen radical etched away loosely bonded carbons and enhance the graphitization of diamond like carbon (DLC) film [39, 40]. Hydrogen radical would etch away disordered carbon atoms such as amorphous carbon rather than graphitic carbon. The bond strength of disordered carbon is weaker than that of ordered carbon.

Fig.4a shows the SEM image of GNS film without hydrogen. A lot of amorphous carbon was deposited on copper substrate and the thickness of graphene sheet observed as increased. The presence of amorphous carbon shown in the film even after equal rates of (1:1) H_2 and C_2H_2 used for deposition (fig. 4b). Highly porous and uniformly distributed GNS observed for the films that used 2:1 ratios of hydrogen and acetylene (fig.4c). The amorphous carbon has been etched out due to the presence of more hydrogen radical in the plasma. If the ratio of

hydrogen still increase, more carbon will etched out and the porous cavity would be increased (fig. 4d).

1.3.2 Morphology of GNS over different substrates

GNS films were deposited over different substrates using plasma enhanced CVD technique. The substrates used for deposition were SiO_2, quarts, SiC, Cu, Pt and Ni. Pt and Ni were sputtered over copper substrate. The average thickness of the coating was about ~40 nm. An amorphous SiC coating was done with reactive sputtering of silicon with acetylene (C_2H_4) over Si substrate and used as the substrate. All the substrates were cleaned with Deionized (DI) water and ultasonicated for 10 minutes. Further the substrates were dried out with dry-air and all the GNS deposition was carried out at a microwave power of 500 W, 12 sccm flow rate of C_2H_2, substrate temperature of 700^0C and 25 min of deposition time. The ratio of the H_2 and C_2H_2 mixture was about 2:1.

The morphology of as deposited GNS over metallic substrates such as, Cu, Pt and Ni was observed by scanning electron microscopy (fig.5). The SEM images show highly porous and vertically aligned thin wall kind of morphology of the GNS electrode, which have large surface to volume ratio. The morphology of NiGNS and PtGNS clearly reveals the spherical flower like graphene petals with 1-2 μm in diameter were uniformly distributed over the surface of the substrate. The graphene walls formed over Ni and Pt coated copper substrates are highly porous and branched (fig.5 c-f), whereas, GNSs over bare copper substrate (fig.5 a & b) are straight with pore size of 50-150nm in diameter.

Fig. 6 shows the SEM image of GNS over insulating substrates such as SiO_2 (fig. 6 a,b), Quartz (fig. 6 c,d) and SiC (fig. 6 e,f). The density of GNS over these substrates were varies. The edges of the vertically grown GNS show highly curled and spiralled. From the SEM images, it is observed that, the nature of substrate has an effect on GNS growth. High density

GNS films were grown over the metallic substrates such as, copper, platinum and nickel. Whereas, the growth of GNS on insulating substrates was observed as less dense. The depositions of GNS over these substrates were performed after the etching the surface in H_2 plasma for 10 min of time. While etching, the surface of Pt and Ni coated copper substrates became very rough. The observed high density GNS over Pt and Ni coated substrates may be due to the effect of roughness.

The cross section views of the CuGNS and PtGNS are shown in fig.7 (a, b). The highly branched morphology of NiGNS and PtGNS offers high surface area and high ratio of porosity. The HRTEM image further shows that number of graphene layers are present in GNS (fig.8b).

Various characterisations were done for the GNS samples. The XRD spectrum of GNS sample has been given in fig. 8a. The peak observed at 2Θ of ~21^0 is assigned as the graphitic peak. The HR-TEM images of graphene flakes are given in fig. 8b. The samples prepared for TEM study was done by scratching the GNS film deposited over cu foil and dispersed in ethanol and ultrasonicated it for 30 minutes. The thick graphite films and thin graphene flakes are dispersed well, wherein few layered light and airy graphene arise to the top. These few layered GNS have been collected and dispersed in ethanol and ultrasonicated for more than 40 min to produce even less few-layered graphene sheets. More than 15 layers of graphene were observed in TEM image.

Raman spectra of GNS film on copper substrate from the initial stage and after the completion of growth was shown in fig. 8c. The spectra clearly shows the graphitizing of the graphene from the amorphous carbon. From the spectra it is observed that amorphous carbon consists in the initial time of synthesis and later it became graphitized. From the Raman

spectra, the G mode (due to bond stretching between pairs of sp^2 carbon atoms) and D mode (due to breathing modes of sp^2 carbon atoms in rings), which lie around 1580 and 1360 cm^{-1} respectively. The D band arises when a finite wave vector mode becomes Raman active in the presence of in plane disorder such as vacancies, stacking faults or finite basal plane dimensions that break translational invariance [41, 42]. The important feature appearing at approximately 2700 cm^{-1} is usually called the 2D-band in the graphite literature and is found in all sp^2 carbon materials. The 2D peak of graphene sheet were emerge in the GNS spectra when compared to the amorphous carbon. 2D peak is used to confirm the presence of graphene and this second order Raman spectrum is due to a double resonance process involving two phonons of opposite wave vector [43]. Second order peaks include both overtones and combinations of first order peaks [44] and are seen at 2700 (2D) and 2930 cm^{-1}(D+G). There is a 13 cm^{-1} blue shift in the G band position when compared to bulk graphite (1581 cm^{-1}) and this shift is attributed to the formation of bulk graphite crystal to graphene sheet [45]. The inset (fig. 8c) shows the Raman spectra from different GNS samples grown on different substrates such as Pt, Ni, Si, SiO_2 and a-SiC after the completion of growth. All the spectra showed clear 2D peak that confirms the graphene growth on all of those substrates.

The high resolution 3D AFM image of GNS has been shown in fig. 8d. The morphology of GNS surface from the AFM image looks same as shown in the SEM images of GNS. The line scan of AFM image on GNS surface gives the details regarding the thickness of the vertically oriented graphene walls as shown in fig. 8e. From the AFM line scan, thickness of each nano wall tip was observed as about 15nm, consists of more than 20 layers of graphene. Carbon-based nanomaterials such as carbon nanotubes and graphene are excellent candidates for super hydrophobic surfaces because of their intrinsically high surface area and nonpolar carbon structure [46]. Theses Nanostructured surface possessing ultrahigh adhesion like Rose

petal effect. Many mechanisms involving to the rose petal effect have been revealed such as morphological factors, composite micro-nanostructure, and chemical defects of hydrophobic surfaces [47- 49]. In order to exhibit the hydrophobic property of graphenen nanosheet matrix, water contact angle (CA) measurement was performed by placing droplet of distilled water on the surface of GNS samples. It was observed that the GNS surface showed strong hydrophobic property. As shown in fig. 8f, the optical image of a water droplet of 2µl gave a CA of 136 ^{0}. The strong hydrophobisity was attributed to the surface roughness induced by morphology of GNS.

Conclusion

Highly porous, vertically oriented graphene nanosheets were synthesised using microwave plasma CVD. These graphene nano structures were shown for strong hydrophobisity. Nanosheets formed on the surface of the substrate and look parallel to the substrate. Each vertically grown nano walls have more than ~15 layers of graphene stacked together. The AFM measurements of the surface of GNS give the wall thickness as approximately 15nm. Much faster growth rate of GNSs was observed in ECR plasma technique. SEM and HR-TEM images reveal the nanosheet formation of carbon and Raman spectra shows defective nature of the film. This plasma CVD synthesis technique for GNS is very much suitable for energy storage as anode for Li thin film batteries.

References

[1] E. Stratakis, S. Savva, D Konios, C Petridi and E Kymakis, *Nanoscale*, 2014, **6**, 6925-6931.

[2] G. Kakavelakis, E. Strataki, D Konios and E Kymakis, *Chemistry of Materials*, 2014, **26**, 5988–5993.

[3] D. Konios, C. Petridis, G. Kakavelakis, M. Sygletou, K.Savva, E. Stratakis and E. Kymakis, *Advanced Funtional Materials*, 2015, **25**, 2213-2221.

[4] N. Balis, D. Konios, E. Stratakis and E. Kymakis, *ChemNanoMat*, 2015, DOI: 10.1002/cnma.201500044.

[5] G. Viskadouros, D. Konios, E. Kymakis, and E. Stratakis, *Applied Physics Letters*, 2014, **105**, 203104.

[6] J. Hassoun, F. Bonaccorso and B. Scrosati et at, *Nano Lett*., 2014, **14**, 4901-4906.

[7] F. Schwierz, *Nanotechnology*, 2010, **5**, 487–496.

[8] C. Chung, Y. K. Kim, D. Shin and D. H. Min et al, *Acc. Chem. Res*., 2013, **46**, 2211-2224.

[9] V. Tozzini and V. Pellegrini, *Phys. Chem. Chem. Phys*., 2013, **15**, 80-89.

[10] D. S. Mao, X. Wang, X. H. Liu, Q. Li and J. F. Xu, *Diamond Relat. Mater*., 2000, **9**, 1876-1880.

[11] C. Berger, Z. Song, X. Li, X. Wu, N. Brown and Naud et al, *Science*, 2006, **312**, 1191-1196.

[12] L. Zhi and K. Mullen, *Mater. Chem*., 2008, **18**, 1472-1484.

[13] A. Reina, X. Jia, J. Ho, D. Nezich, H. Son and V. Bulovic et al, *Nano Lett*., 2009, **9**, 30-35.

[14] S. J. Park and R.S. Ruoff, *Nat. Nanotechnology*, 2009, **4,** 217-224.

[15] S. Bae, H. Kim and S. Iijima et al, *Nat. Nanotechnol*., 2010, **5**, 574-578

[16] M. Yi and Z. shen, *J. Mater. Chem. A*, 2015, **3**, 11700-11715.

[17] W. S. Hummers, and R. E. Fffeman, *J. Am. Chem. Soc*., 1958, **80**, 1339-1339.

[18] Y. Hernandez, V. Nicolosi and J. N. Coleman et al, *Nat. Nanotechnol*., 2008, **3**, 563-568.

[19] K. V. Emtse, A. Bostwick and T. Seyller et al, *Nat. Mater*., 2009, **8**, 203-207.

[20] S. Gilje, S. Han, K. L. Wang and R. B. Kaner, *Nano Lett.*, 2007, **7**, 3394 -3398.

[21] R. Thomas, G. M. Rao, *Electrochimica Acta*, 2014, **125**, 380–385.

[22] R. Thomas, K. Y. Rao, G. M. Rao, *Electrochimica Acta*, 2013, **108,** 458– 464.

[23] B. Y. Yang, J. Chen, K. Yu, J. Yan and K. Cen, *Nanoscale*, 2013, **5**, 5180-5204.

[24] Y. Y. Wang, S. Gupta and R. J. Nemanich, *Appl. Phys. Lett*., 2004, **85**, 2601-2603.

[25] Y. Wu, P. Qiao, T. Chong and Z. Shen, *Adv. Mater*., 2002, **14**, 64-67.

[26] S. Virendra, J. Daeha, Z. Lei, D. Soumen, I. K. Saifal and S. Sudipta, *Progress in Materials Science*, 2011, **56**, 1178-1271.

[27] R. Vitchev, A. Malesevic, R.H. Petrov, R. Kemps, M. Mertens and A. Vanhulsel et al, *Nanotechnolgy*, 2010, **21**, 095602 (1-8).

[28] K.V. Deenamma and G. M. Rao, *Rev. Sci. Instr*., 2000, **71**, 467-471.

[29] K. Yu, Z. Bo, G. Lu, S. Mao, S. Cui, Y. Zhu, X. Chen, R. S. Ruoff and J. Chen, *Nanoscale Res. Lett*., 2011, **6**, 202 (1-9).

[30] K. Yu, P. Wang, G. Lu, K. H. Chen, Z. Bo and J. Chen, *J. Phys. Chem. Lett*., 2011, **2**, 537 -542.

[31] Z. Bo, K. Yu, G. Lu, S. Cui, S. Mao and J. Chen, *Energy Environ. Sci*., 2011, **49**, 1849-1858.

[32] Y. Wu, P. Qiao, T. Chong, and Z. Shen, *Adv. Mater*. 2002, **14**, 64-67.

[33] Y. Wu, *Nano Letter*, 2002, **2**, 355-359.

[34] S. H. Tsai, C. W. Chao, C. L. Lee, and H. C. Shih, *Appl. Phys. Lett*. 1999, **74**, □3462.

[35] C. Bower, W. Zhu, S. Jin and O. Zhou, *Appl. Phys. Lett*. , 2000, **77**, 830.

[36] Z. Wang, M. Shoji and H. Ogata, *Applied Surface Science*, 2011, **257**, 9082-9085.

[37] A. Ural, Y. M. Li and H. J. Dai, *Appl. Phys. Lett*., 2002**, 81**, 3464-3466.

[38] Y. Wu and B. Yang, *Nano Lett.*, 2002, **2**, 355-359.

[39] S. Shimabukuro, Y. Hatakeyama, M. Takeuchi, T. Itoh and S. Nonomura, *Thin Solid Films*, 2008, **516**, 710-713.

[40] C. L. Cheng, C. T. Chia, C. C. Chiu and I. N. Lin, *Diamond Relat. Mater.,* 2002, **11**, 262-267.

[41] Z. H. Ni, H. M. Fan, Y. P. Feng, Z. X. Shen, B. J. Yang and Y. H. Wu, *J. Chem. Phys*., 2006, **124**, 204703 (1-5).

[42] R. Saito, A. Jorio, A. G. S. Filho, G. Dresselhaus, M. S. Dresselhaus, M. A. Pimenta, *Phys. Rev. Lett.*, 2001, **88**, 027401(1-4).

[43] M. S. Dresselhaus, G. Dresselhaus and M. Hofmann, *Phil. Trans. R. Soc*., 2008, **A 366**, 231-236.

[44] R. J. Nemanich and S. A. Solin, *Phys. Rev. B*, 1979, **20**, 392-401.

[45] M. A. Pimenta, G. Dresselhaus, M. S. Dresselhaus, L. A. Cancado, A. Jorio, R. Sato, *Phys. Chem. Chem. Phys*., 2007, **9**, 1276-1291.

[46] Y. Lin, G. J. Ehlert, C. Bukowsky and H. A. Sodano , *ACS Appl. Mater. Interfaces*, 2011, **3**, 2200-2203.

[47] B. Bhushan and E. K. Her, *Langmuir*, 2010, **26**, 8207-8217.

[48] M. J. Liu and L. Jiang, *Advanced Functional Materials*, 2010, **20**, 3753-3764.

[49] F. M. Chang, S. J. Hong, Y. J. Sheng, and H. K. Tsao, *Appl. Phys. Lett*., 2009, **95**, 064102 (1-3).

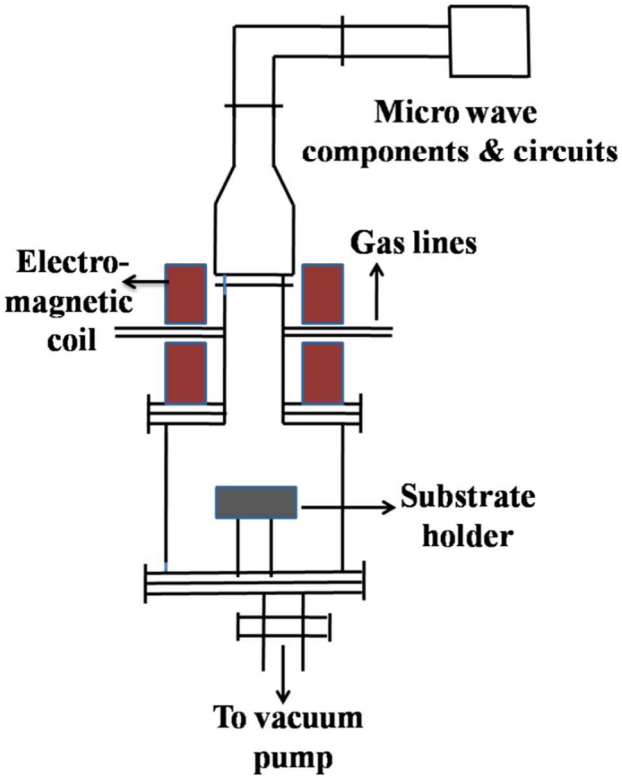

Fig. 1 Schematic of ECR plasma CVD setup

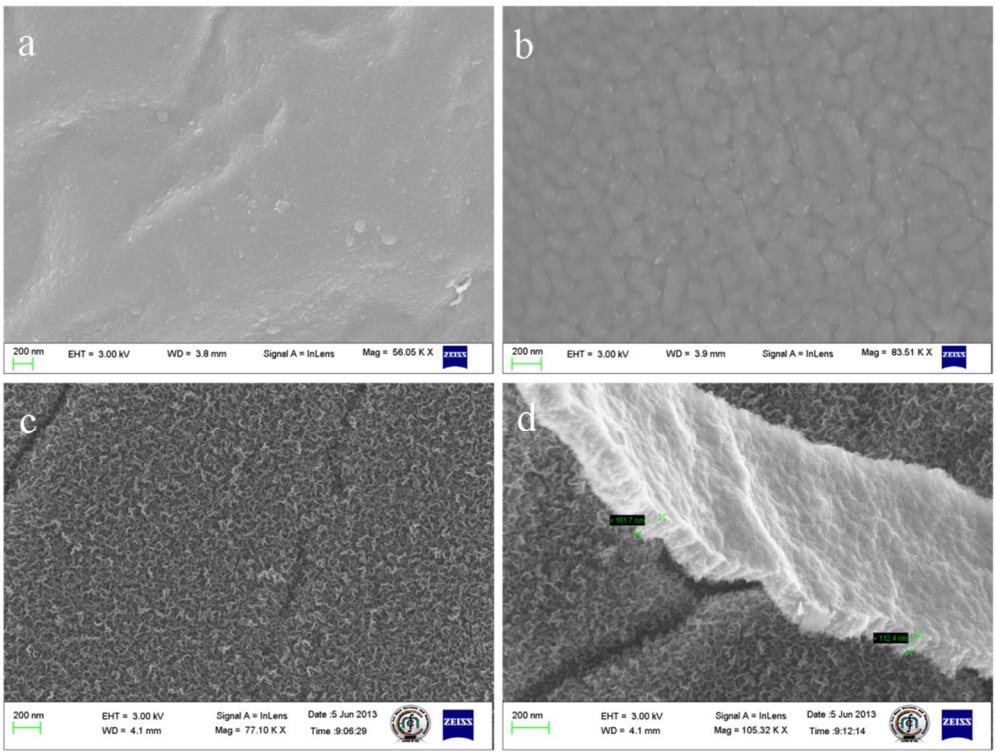

Fig. 2 SEM image of graphene nanosheet grown on Cu substrate by ECR-PECVD (a) at 1min of deposition, (b) at 3min of deposition and (c) at 5min of deposition. (d) Thickness of GNS. (All deposition was carried out at 500W microwave power, 700^0C and C_2H_2:H_2 = 1:2)

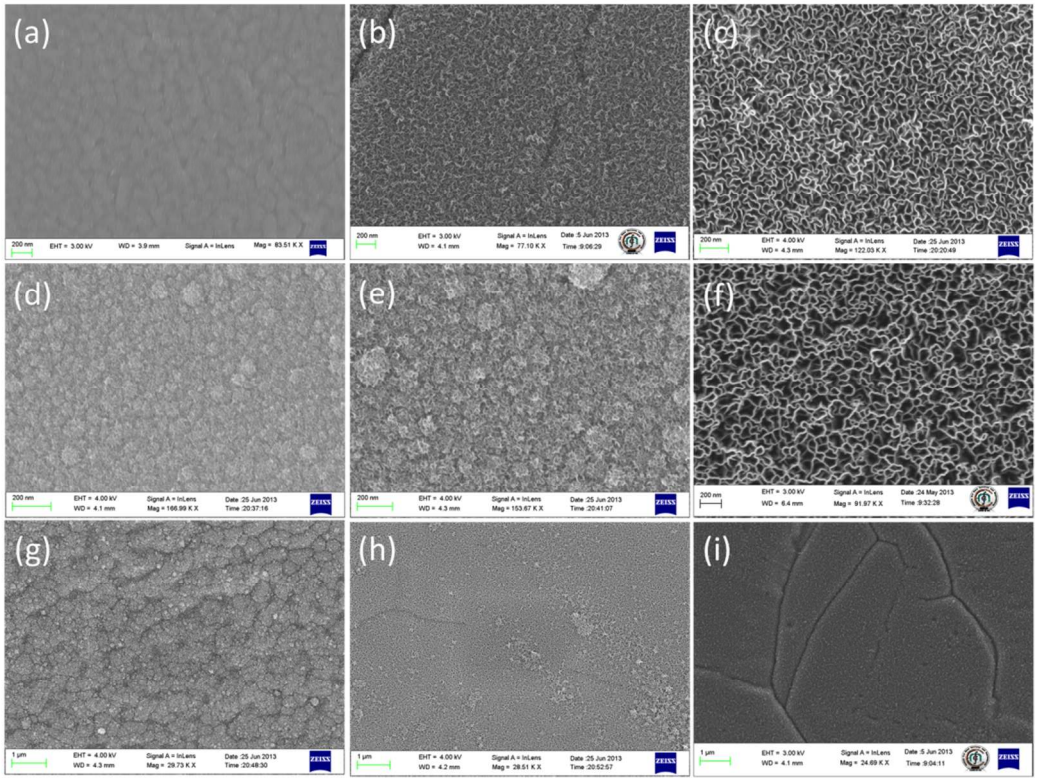

Fig. 3 SEM images of GNS on Cu substrate at various flow rate of C_2H_2 (a) at 5 sccm, (b) at 12 sccm (c) at 25 sccm, at various microwave power (d) at 100W, (e) at 200W and (f) at 500W, at various temperature (g) at room temperature, (h) at 400^0C and (i) at 700^0C.

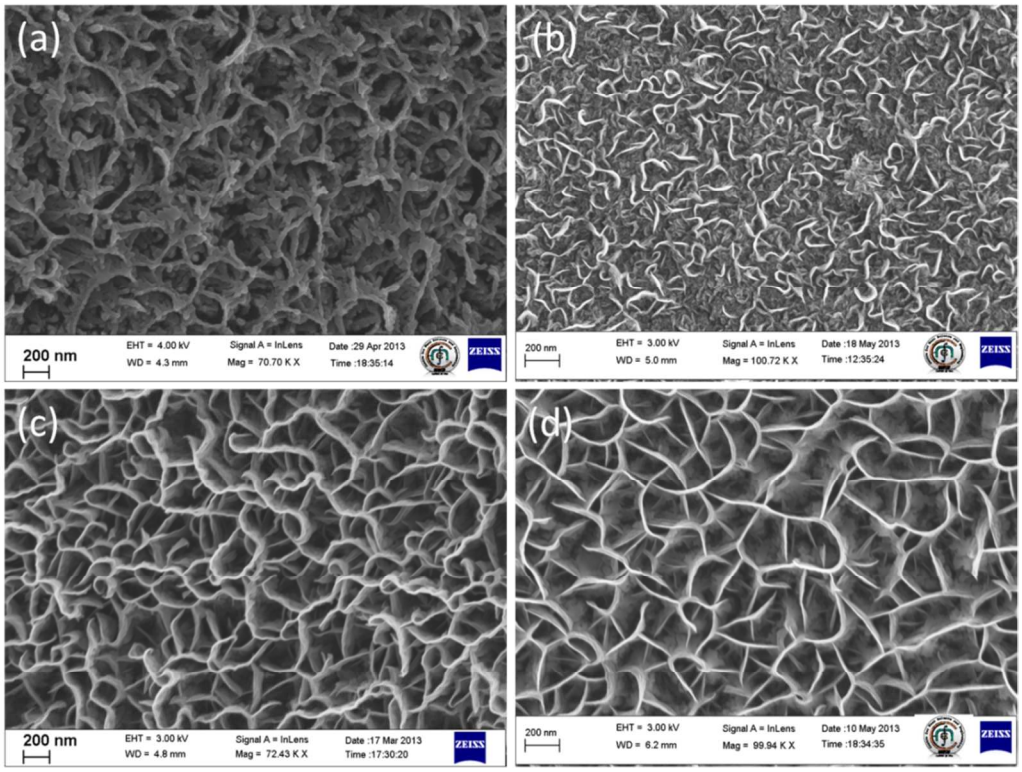

Fig. 4 SEM images of GNS at various hydrogen dilution with C_2H_2 (a) without hydrogen, (b) at H_2:C_2H_2**;** 1:1 (c) H_2:C_2H_2**;** 2:1 And (d) H_2:C_2H_2**;** 3:1 (all deposition was carried out at 12sccm of C_2H_2, 500W and 20 minutes of deposition time, 700^0C)

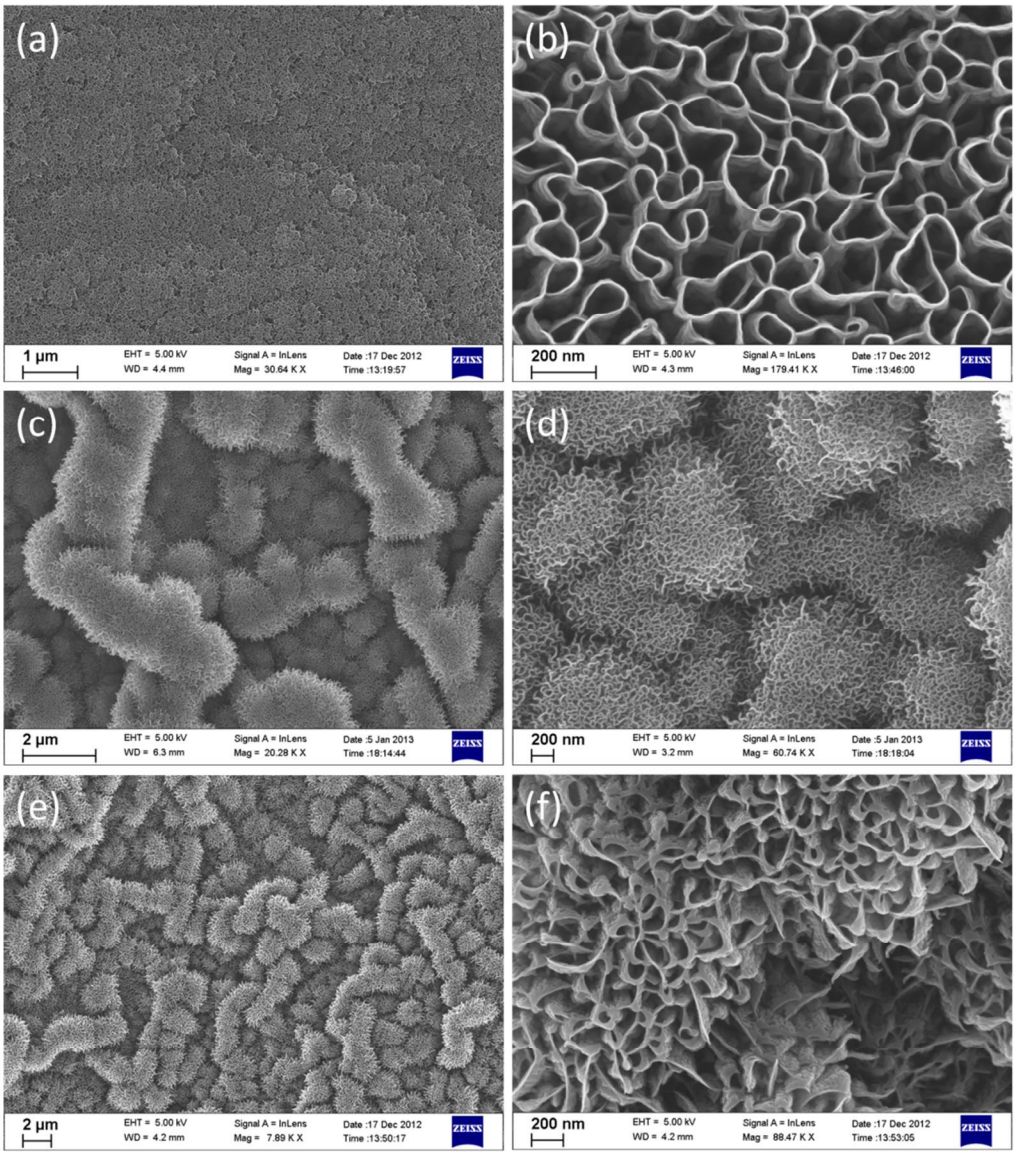

Fig. 5 scaning electron microscope (SEM) image of graphene nano sheet on (a, b) copper, (c, d) nickel and (e, f) platinum substrates.

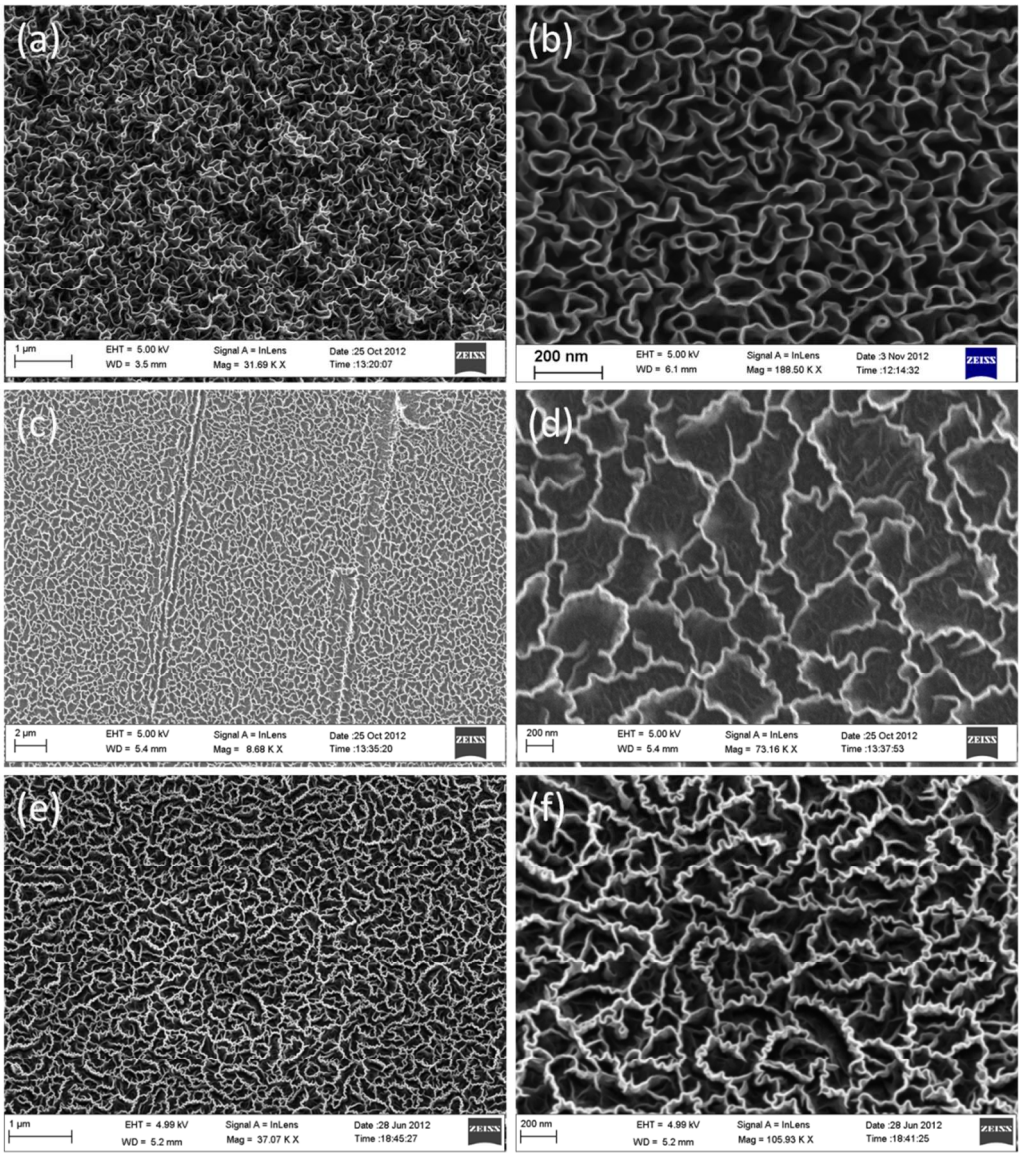

Fig. 6 SEM image of GNS on (a, b) SiO2, (c,d) quartz and (e,f) SiC substrates.

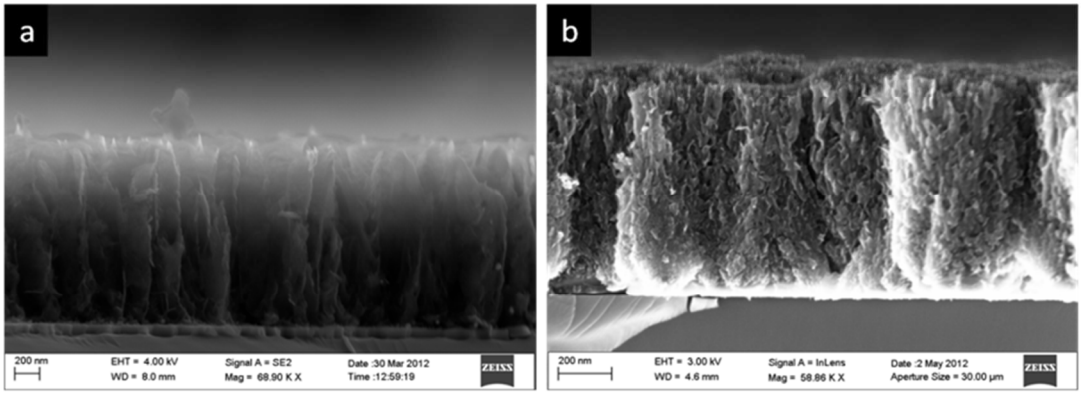

Fig. 7 Cross section view of grapene nanosheet (a) PtGNS, which is highly branched and vertically grown and (b) CuGNS electrode, aligned vertically and straight forward.

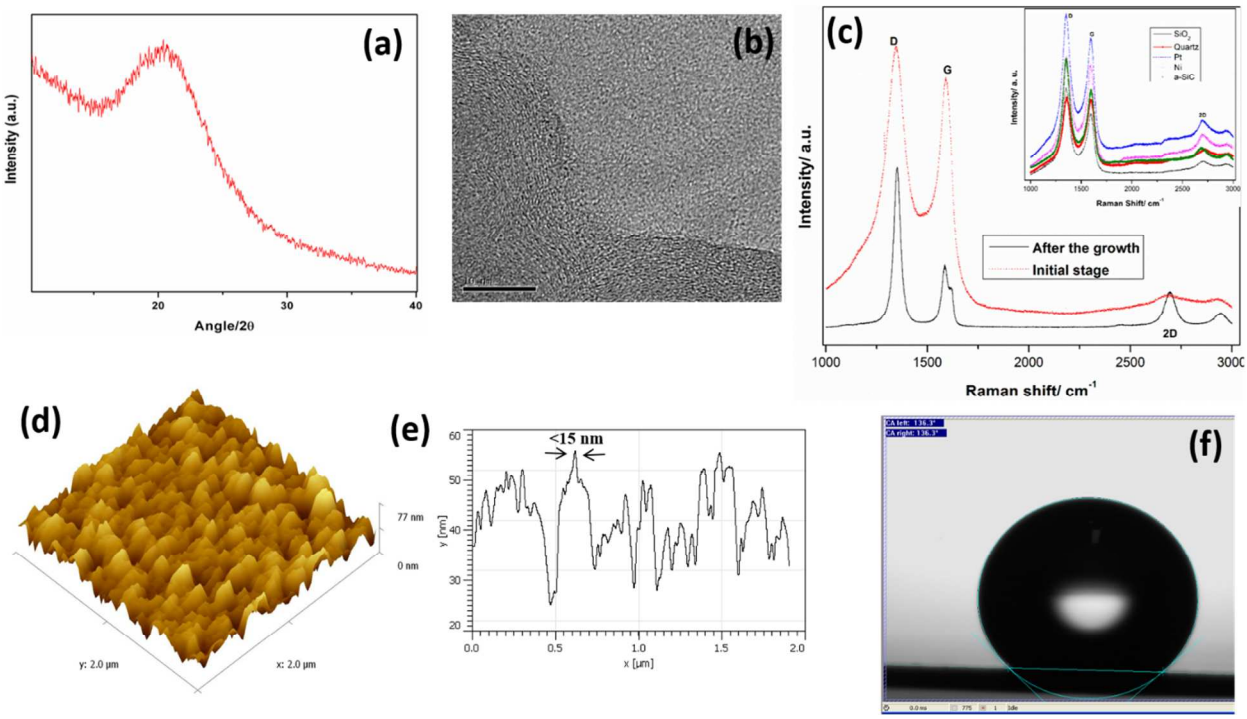

Fig. 8 various characterizations for GNS are shown in the figure. (a) XRD spectrum (b) HR-TEM image (c) Raman spectra of GNS on Cu substrate (inset: spectra of GNS on different substrates) (d) 3d AFM image (e) The line spectra from the AFM image and (f) The contact angle measurement on GNS surface.